Correspondence

Modeling an Asynchronous Data Echo Canceller

O. MACCHI AND S. MARCOS

Abstract—**In this paper, we show that an adaptive echo canceller with asynchronous inputs affected by sampling time jitter can be modeled as the identification of a time-varying channel by an adaptive filter, both the channel and the adaptive filter being fed with synchronous data. This allows to apply theoretical results of the identification problem which are already known. We prove that the problem is similar when the transmitter itself is slaved on an external jittered clock and the echo canceller is synchronous.**

I. Introduction

In two-wire full duplex data transmission, the far-end received signal is disturbed by an echo of local data reflected at impedance mismatches. An adaptive digital echo canceller (EC), as shown in Fig. 1, will estimate the echo path impulse response, pass the (known) local symbols through this estimated path and subtract the resulting output from the far-end received signal.

This paper deals with an asynchronous EC. This is not a classical problem. In a recent paper [1], Falconer addressed the problem within the framework of digital subscriber loops. In this case, the transmitter is slaved on the central terminal clock. At a distant station, the latter is recovered with jitter but the EC input remains at a (synchronous) local symbol rate $1/T_b$. This model, denoted F, is depicted in Fig. 2. The randomly jittered times at which symbols are transmitted create naturally fluctuations in the true echo; these fluctuations cannot be suitably identified by the adaptive EC and after subtraction the residual echo is increased. Note that two interesting methods have been proposed to cancel this residual echo due to jitter [2], [3].

Here, we address a slightly different problem [4]. As it is assumed that the EC is slaved on the central terminal clock which is recovered with jitter, the EC input as well as the received signal are sampled in an asynchronous manner. It is important to note that to use the EC in this way, the input near-end signal must be oversampled at a Nyquist sampling rate $1/T_s > 1/T_b$, in order to build the echo replica from the asynchronous input data. This is not generally required for a classical EC with synchronous inputs. To achieve the over-sampling, the near-end data must thus be shaped (at least partly) by the transmitter into an analog signal prior to entering the EC. This model, denoted M, is depicted in Fig. 1.

Section II establishes a theoretical synchronous model, denoted T, which is equivalent to both practical models F and M of the asynchronous EC. It is shown that the problem can always be viewed as a standard adaptive identification of a linear but nonstationary (time-varying) echo path, both the true filter and the adaptive one being fed with synchronous data. This is not obvious since the jitter effects in the filter inputs are not linear. The practical interest of our modeling is explained in Section III. While Falconer puts emphasis on the spectral analysis of the residual echo due to jitter, the equivalent synchronous model provides an analysis for the EC ability to track the time jitter.

Paper approved by the Editor for Channel Equalization of the IEEE Communications Society. Manuscript received August 18, 1987; revised January 25, 1988. This paper was presented at EUSIPCO '86, The Hague, The Netherlands, September 2-5, 1986.

The authors are with the Laboratoire des Signaux et Systemes, CNRS-ESE, 91190 GIF sur YVETTE, France.

IEEE Log Number 8824906.

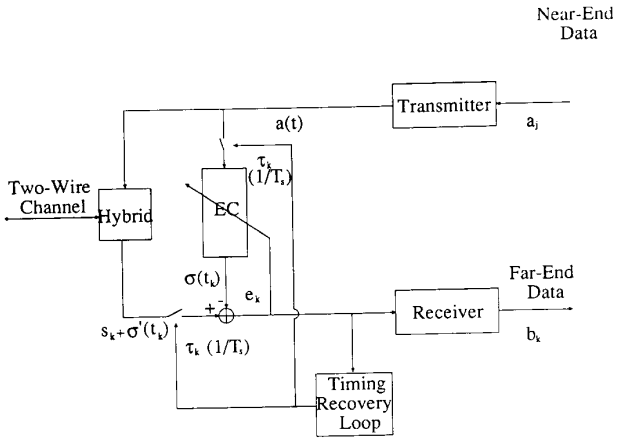

Fig. 1. Model M: An asynchronous echocanceller (EC).

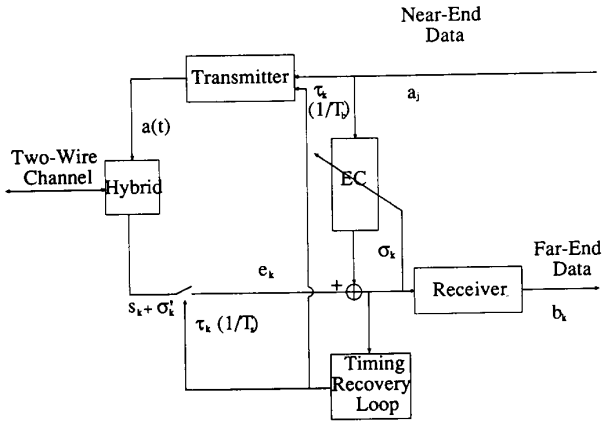

Fig. 2. Model F (cf. [1]).

II. A Nonstationary Model

A. Analysis of Model M

The relevant system is depicted in Fig. 1. In model M, at each step the timing recovery loop gives the phase τ_k used to sample, on the one hand the analog signal $a(t)$ entering the EC, and on the other hand, the received signal $x(t)$ delivered by the hybrid. Due to additive noise and residual echo after the EC, the timing loop recovers the instant

$$t_k = kT_s + \tau_k \tag{2-1}$$

where τ_k is the time jitter and $1/T_s$ is a Nyquist sampling rate satisfying Shannon's theorem. This rate is greater than the

symbol rate $1/T_b$, but the EC must be worked at an oversampled rate. If the EC input data signal were sampled with the (jittered) recovered symbol rate clock, some symbols might be forgotten in the reconstruction of the echo replica. For mathematical derivation, the same sampling instant (2-1) is used to sample the analog signal at the receiver input, which is written

$$\sigma'(t) = a(t) * c(t) = \int_{-\infty}^{+\infty} a(u)c(t-u)\,du. \quad (2\text{-}2)$$

In this equation, $c(t)$ is the analog echo path response and $a(t)$ is the analog data signal transmitted on the line, $(*)$ denoting the convolution operator.

The equivalence between analog convolutions and digital convolutions at the Nyquist rate are well known, namely,

$$\sigma'(t) = T_s\Sigma_l a(lT_s)c(t-lT_s) = T_s\Sigma_l c(lT_s)a(t-lT_s). \quad (2\text{-}3)$$

Hence, at time t_k, the echo and its replica are, respectively,

$$\sigma'(t_k) = T_s\Sigma_l c(lT_s)a((k-l)T_s+\tau_k) \quad (2\text{-}4)$$

$$\sigma(t_k) = \Sigma_l c_k(l)a[(k-l)T_s+\tau_{k-l}] \quad (2\text{-}5)$$

where $c_k(l)$ is the lth coefficient of the adaptive EC at time t_k. The jitter τ_k can be assumed to be much less than T_s, hence, the first-order approximations

$$\sigma'(t_k) = T_s\Sigma_l c(lT_s)\{a((k-l)T_s)+\tau_k\dot{a}((k-l)T_s)\} \quad (2\text{-}6)$$

$$\sigma(t_k) = \Sigma_l c_k(l)\{a((k-l)T_s)+\tau_{k-l}\dot{a}((k-l)T_s)\} \quad (2\text{-}7)$$

where $\dot{x}$ denotes the derivative of x. The residual echo is thus

$$\begin{aligned}\sigma'(t_k)-\sigma(t_k) = {} & \Sigma_l(T_s c(lT_s)-c_k(l))a[(k-l)T_s] + \\ & + \Sigma_l T_s c(lT_s)(\tau_k-\tau_{k-l})\dot{a}[(k-l)T_s] \\ & + \Sigma_l \tau_{k-l}(T_s c(lT_s)-c_k(l))\dot{a}[(k-l)T_s].\end{aligned} \quad (2\text{-}8)$$

The first term of the RHS of (2-8) is the residual echo in the jitter-free case while the two others are residuals due to the jitter. The third term is of second order in comparison to the first term.

To derive the theoretical model $\boldsymbol{T}$, we now introduce the fictitious echo and its replica according to

$$\sigma'_{1,k} = T_s\Sigma_l c(lT_s)a[(k-l)T_s+\tau_k-\tau_{k-l}], \quad (2\text{-}9)$$

$$\sigma_{1,k} = \Sigma_l c_k(l)a[(k-l)T_s]. \quad (2\text{-}10)$$

Once the second-order error has been dropped in (2-8), it clearly follows that

$$\sigma'_{1,k}-\sigma_{1,k} = \sigma'(t_k)-\sigma(t_k); \quad (2\text{-}11)$$

so this model has the same residual echo as the true practical model $\boldsymbol{M}$. Equations (2-9), (2-10) describe an invariant echo path $c(t)$ fed with jittered data, whereas the EC input is synchronous. The model is only fictitious because all the past data samples $a[(k-l)T_s+\tau_k-\tau_{k-l}]$ entering the echo path and appearing in (2-9) are not only delayed at each new step k, but need to be readjusted in time due to the jitter term τ_k. But this will greatly help our analysis of model $\boldsymbol{M}$.

B. Derivation of Model T

Since the sampling rate $1/T_s$ is higher than the symbol rate $1/T_b$, we shall distinguish a number $M = T_b/T_s$ of sampling phases; M can be assumed integer. The time indexes k and n corresponding to the respective clocks $1/T_s$ and $1/T_b$ are related through

$$kT_s = nT_b + mT_s \quad 0 \le m \le M-1. \quad (2\text{-}12)$$

If $\alpha(t)$ denotes the analog shaping filter response, the analog signal $a(t)$ delivered by the transmitter at the echo path input (and at the EC input) is

$$a(t) = \Sigma_q a_q \alpha(t-qT_b) \quad (2\text{-}13)$$

where the a_q are the synchronous data transmitted at the symbol rate. Replacing (2-13) in (2-9) and (2-10), it is shown in the Appendix that

$$\sigma'_{1,k} = A_n^T G^{m,n} \quad (2\text{-}14)$$

$$\sigma_{1,k} = A_n^T H^{m,n} \quad (2\text{-}15)$$

where

$$A_n = (a_{n+N}, \cdots, a_n, \cdots, a_{n-N})^T \quad (2\text{-}16)$$

is the data vector at time nT_b, $(2N+1)$ being the length of the echo path in symbol periods. The M vectors

$$G^{m,n} = (g^{m,n}_{-N}, g^{m,n}_{-N+1}, \cdots, g^{m,n}_0, \cdots, g^{m,n}_N)^T, \quad m = 0, \cdots, M-1 \quad (2\text{-}17)$$

represent at time nT_b the M phases of a time-varying echo path, each phase being sampled at the symbol rate. These time variations are consequences of the time jitter. Their exact expression is given in (A-3). Naturally, when interleaved, these M vectors constitute the impulse response of a time-varying echo path sampled at the Nyquist sampling rate. The corresponding large vector G_k has its $M(2N+1)$ coefficients satisfying

$$g_k(j) = g^{m,n}_p \quad \text{for } jT_s = pT_b + mT_s \quad (2\text{-}18)$$

and it follows from the Appendix that

$$g_k(j) = T_s\Sigma_l c(lT_s)\alpha[(j-l)T_s+\tau_k-\tau_{k-l}]. \quad (2\text{-}19)$$

These values are the samples for all times jT_s of an echo path changing with time k. This path is jitter distorted (due to τ) and includes the transmitter shaping filter $\alpha(t)$ together with the echo channel $c(t)$ itself.

Finally, in (2-15), the M echo cancellers

$$H^{m,n} = (h^{m,n}_{-N}, h^{m,n}_{-N+1}, \cdots, h^{m,n}_0, \cdots, h^{m,n}_N)^T, \quad m = 0, \cdots, M-1 \quad (2\text{-}20)$$

thanks to the shaping filter, are linearly related to the adaptive coefficients $c_k(l)$ of the oversampled EC of our practical model $\boldsymbol{M}$ [cf. (2-5)]. Namely, one has

$$h_k(j) = h^{m,n}_p \text{ for } jT_s = pT_b + mT_s \quad (2\text{-}21)$$

where the

$$h_k(j) = \Sigma_l \alpha(lT_s)c_k(j-l) = \Sigma_l c_k(l)\alpha[(j-l)T_s] \quad (2\text{-}22)$$

are the coefficients of the large interleaved vector H_k built up with the $H^{m,n}$ like G_k in (2-18). The model (2-14), (2-15) is equivalent to our practical model $\boldsymbol{M}$ given in (2-4), (2-5) where both the echo and its replica are distorted by jitter. But there are three major differences. *First, there is no more oversampling, the sampling rate at the input of both the echo path and the EC is the symbol rate. Second, these input data symbols are synchronous. Third, all the jitter effects are carried on by the echo line.* Hence, system $\boldsymbol{M}$ can be modeled by model $\boldsymbol{T}$ depicted in Fig. 3 where for simplification we have dropped the index m of the sampling

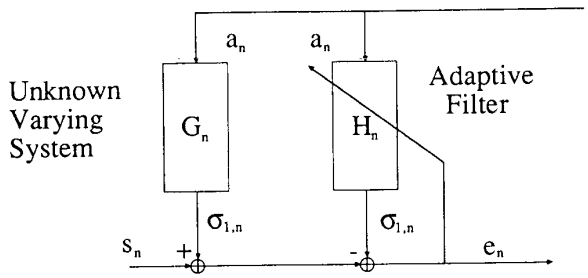

Fig. 3. Model T: Identification of a time-varying system.

phase. Each phase is worked independently in model T. This model clearly describes identification of the time-varying filter G_n by the adaptive filter H_n fed with a synchronous rate, as theoretically studied in [5]–[7].

To conclude this section, let us emphasize the similarity of our model with that of Falconer. In [1], the distortion acts upon the channel impulse response [see [1], eq. (6-a), (7)] in such a way that the echo is also given by (2-14) but with coefficients

$$g_p^{m,n} = G(pT_b + mT_s + \tau_n^m - \tau_{n-p}^m). \tag{2-23}$$

(In (2-23) the jitter τ_k has been written τ_n^m to make apparent the label n of the baud interval). Taking into account that in model F (respectively, M) the jittered clock is introduced before (respectively, after) the shaping filter $\alpha(t)$, formula (2-23) of Falconer is exactly the same as (2-18), (2-19) in our model. In summary, the asynchronous practical situation of time jitter discussed in [1] (model F) and the one discussed in the present paper (model M) are equivalent to the classical adaptive identification of a time-varying channel with synchronous timing.

III. Practical Interest of the Modeling

The previous result is important in practice because model T has tracking capability. It is indeed well-known [5]–[7] that the classical least mean square (LMS) algorithm has an optimum step-size which minimizes the misadjustment between the parameters of the EC and those of the varying system to be identified. It compromises between the fluctuations due to the stochastic approximation in the algorithm increment and the time variations due to jitter. This has been derived in particular in [7] both for the case (R) of random zero-mean increments (see equation IV.5), and for case (D) of deterministic bounded increments (see equation IV.10). The optimum step size depends on the EC length, the input signal and noise powers, and on the parameters

$$\text{case } (R) \qquad d_R^2 = E[|G_{n+1} - G_n|^2], \tag{3-1}$$

$$\text{case } (D) \qquad d_D^2 = \text{Sup}_n \{|G_{n+1} - G_n|^2\}, \tag{3-2}$$

which are related to the time increments of the nonstationary echo path G_n to be identified. The parameter d_R^2 (or d_D^2) can be easily derived. Using (2-17) and (2-19), we obtain for a fixed phase m

$$d_R^2 = E[\Sigma_p |g_p^{n+1} - g_p^n|^2] = E[\Sigma_{j=Mp} |g_{k+M}(j) - g_k(j)|^2] \tag{3-3}$$

where $g_k(j)$ is given in (2-19) and similarly for d_D^2 with the supremum. With a first-order approximation based on $\tau_k - \tau_{k-l}$ much less than T_s, it yields

$$d_R^2 = \Sigma_p \Sigma_{l,j} T_s^2 c(lT_s) c(jT_s) \dot{\alpha}[(Mp - l)T_s] \cdot \dot{\alpha}[(Mp - j)T_s] E[\delta_n(l)\delta_n(j)] \tag{3-4}$$

where

$$\delta_n(l) = \tau_{k+M} - \tau_{k+M-l} - \tau_k + \tau_{k-l} = \tau_{n+1} - \tau_{n+1-l} - \tau_n + \tau_{n-l} \tag{3-5}$$

according to relation (2-12) between the indexes k and n. Similarly, in the deterministic case, with the same definition of $\delta_n(l)$, one gets

$$d_D^2 = \Sigma_p |T_S \Sigma_l c(lT_s) \dot{\alpha}[(Mp - l)T_s] \text{ Sup}_n \delta_n(l)|^2. \tag{3-6}$$

The simulations are done according to the asynchronous model (2-4) and (2-5), corresponding to model M depicted in Fig. 1. The (baseband) echo path and the transmitter spectral shaping are

$$\alpha(t) = c(t) = (\sin(\pi t/T_b)/\pi t/T_b) \cdot (\cos(\lambda_0 \pi t/T_b)/(1 - 4\lambda_0^2 t^2/T_b^2) \tag{3-7}$$

with $1/T_b = 2400$ Hz, $\lambda_o = 1/6$, $M = 3$. The jitter is of sinusoidal form

$$\tau_n/T_b = \lambda \sin(2\pi f_0 n T_b) \tag{3-8}$$

repeated M ($M = 3$) times during the symbol period. A similar model already used in [8] corresponds to a cyclostationary signal like data echo (or residual echo) entering the timing recovery loop. With the aim of analyzing the tracking capability of the LMS algorithm, the results of model M in this case (3-7), (3-8), were presented in the recent [7] where Fig. 3 corresponds to $f_o = 0.5$ Hz and $\lambda = 3.10^{-2}$. But the same simulation results can also be used to illustrate that our theoretical equivalent model T is quite satisfactory and efficient. The model (3-8) of jitter can be viewed as random by averaging over time rather than over set trials. Then, with definition (3-5) one gets

$$E[\delta_n(l)\delta_n(j)] = 8\lambda^2 T_b^2 \sin^2(\pi f_o T_b) \sin(\pi f_o l T_b/3) \cdot \sin(\pi f_o j T_b/3) \cos(\pi f_o (l-j) T_b/3). \tag{3-9}$$

After replacing the sine and cosine functions in (3-9) by their first-order approximations, the general expression (3-4) becomes

$$d_R^2 = 8\lambda^2 T_b^2 (\pi f_0 T_b)^2 (\pi f_0)^2 \Sigma_p |f(pT_b)|^2 \tag{3-10}$$

with

$$f(pT_b) = \Sigma_l T_s c(lT_s) \alpha[(3p - l)T_s] l T_s. \tag{3-11}$$

The model (3-8) of jitter can also be viewed as deterministic, but now d_D^2 is only an upper bound. After some manipulations we obtain

$$d_D^2 = 2 d_R^2. \tag{3-12}$$

The complex symbols corresponding to 16 state QAM are encoded into the real emitted signal $a(t)$ through the spectral shaping $\alpha(t)$ and modulation with barrier $\upsilon_o = 1800$ Hz. The analog signal $a(t)$ then enters both the echo path and the EC. The EC has 63 T_s-spaced real taps. To obtain the echo signal we sampled the function (3-7) at the rate $1/T_s = 7200$ Hz and made the convolution with the symbol sequence. The EC input is generated in the same way by sampling (3-7) at rate $1/T_s$ and at phase τ_n. The echo path has also been modulated. The far-end signal is obtained in the same way.

The results given in Fig. 4(a), (b) were obtained in the same conditions with $f_o = 0.5$ Hz and $\lambda = 3.10^{-2}$. They illustrate the influence of the step size of the algorithm on the jitter effects. Note that the ratio ϵ/P of residual echo to initial echo power is a squared sine-wave like τ_n^2. But as μ is increased to $\mu = 2^{-10}$, this residual jitter is smoothed out. By analogy with

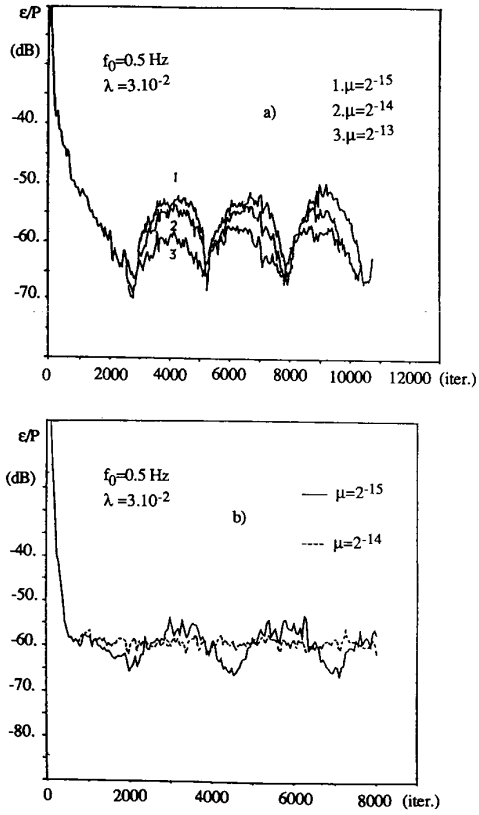

Fig. 4. Influence of μ on the jitter effects.

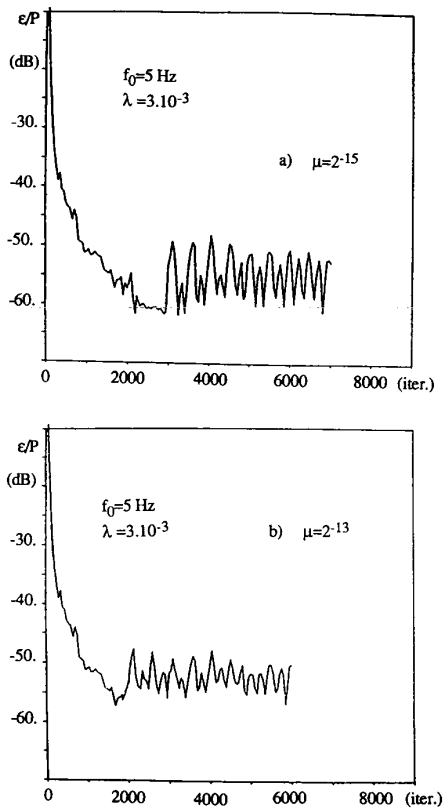

Fig. 5. Influence of μ on the high-frequency jitter effects.

the model T, the conclusion is that the adaptive EC fed with jittered inputs can compensate some of the jitter effects with an appropriate choice of the step size. The results of Fig. 5(a), (b) show the same capacity to compensate for a part of the jitter, but at the higher frequency $f_o = 5$ Hz.

On the other hand, the analysis in [1] states that roughly

$$\epsilon/P = |\tau_n - \tau_{n-1}|/T_b$$

(-44 dB in our two cases $f_o = 0.5$ Hz, $\lambda = 3.10^{-2}$ and $f_o = 5$ Hz, $\lambda = 3.10^{-3}$) and that the maximum acceptable jitter frequency is $f_o = \mu/T_b$. In the case where $\mu = 2^{-15}$, this analysis would yield $f_o = 0.1$ Hz, whereas we find the better result $\epsilon/P = -58$ dB for $f_o = 0.5$ Hz and still obtain the satisfactory result $\epsilon/P = -55$ dB for the more rapid jitter $f_o = 5$ Hz. The analysis in [1] is thus a bit pessimistic. It does not in fact take into account the tracking capability of the algorithm and computes the lag error as if the EC were fixed at the constant (jitter free) value of the echo path. This is presumably the reason.

VI. Conclusion

The problem of an echo canceller called asynchronous in the sense that its inputs are slaved on a jittered timing recovery circuit has been shown to be equivalent to the problem of identifying a nonstationary echo path using an adaptive system when the true echo path and the adaptive canceller are both fed with synchronous data. A slightly different problem addressed by Falconer has been proved to be similar. This modeling allows the analysis of the performances of such asynchronous EC by applying known theoretical results about adaptive identification in a nonstationary environment. This modeling shows in particular that an adaptive EC with jittered inputs can compensate for jitter effects by choosing an appropriate step-size.

Appendix

Derivation of Model T

We use the indexes j, k, for the fast clock $1/T_s$ and indexes n, p, q for the slow clock $1/T_b$. Finally, m will designate a sampling phase among the M possible ones as in (2-12). Substituting (2-13) into (2-9) the echo becomes

$$\sigma'_{1,k} = T_s \Sigma_l \Sigma_q c(lT_s) a_q \alpha[(k-l)T_s - qT_b + \tau_k - \tau_{k-l}]$$
$$= \Sigma_q a_q T_s \Sigma_l c(lT_s) \alpha[(k-l)T_s - qT_b + \tau_k - \tau_{k-l}]. \quad \text{(A-1)}$$

Using the representation (2-12) of kT_s and using the index $p = n - q$, (A-1) yields

$$\sigma'_{1,k} = \Sigma_p a_{n-p} g_p^{m,n} \quad \text{(A-2)}$$

with the help of the coefficients

$$g_p^{m,n} = T_s \Sigma_l c(lT_s) \alpha(pT_b + mT_s - lT_s + \tau_k - \tau_{k-l})$$
$$p = -N, -N+1, \cdots, N, \quad \text{(A-3)}$$

index n is contained in k through (2-12). Clearly, (A-2) is equivalent to the scalar product (2-14) of the data vector A_n (at the baud rate) with vector $G^{m,n} = (g_{-N}^{m,n}, \cdots, g_N^{m,n})^T$. This vector changes when k changes, due to the jitter variations $\tau_k - \tau_{k-l}$. Note that the M vectors $G^{m,n} (m = 0, \cdots, M-1)$ are the M phases of a larger vector G_k with time adjacent coefficients $g_k(j)$ given at the Nyquist rate according to

$$g_k(j) = g_p^{m,n} \quad \text{when } jT_s = pT_b + mT_s. \quad \text{(A-4)}$$

This interleaving yields a simple formula for the time-varying

echo path at the Nyquist rate, namely,

$$g_k(j) = T_s \Sigma_l c(lT_s)\alpha[(j-l)T_s + \tau_k - \tau_{k-l}]. \quad \text{(A-5)}$$

Putting (2-13) into (2-10), it is also easy to show that the echo replica is

$$\sigma_{1,k} = \Sigma_p a_{n-p} \Sigma_l c_k(l)\alpha(pT_b + mT_s - lT_s) \quad \text{(A-6)}$$

$$= A_n^T H^{m,n} \quad \text{(A-7)}$$

where the M vectors $H^{m,n}(m = 0, \cdots, M-1)$ are defined by (2-21) and correspond to M interleaved EC's.

REFERENCES

[1] D. Falconer, "Timing jitter effects on digital subscriber loop echo cancellers: Part I," *IEEE Trans. Commun.*, vol. COM-33, pp. 826–832, Aug. 1985.

[2] D. G. Messerschmitt, "Asynchronous and timing jitter insensitive data echo cancellation," *IEEE Trans. Commun.*, vol. COM-34, pp. 1209–1217, Dec. 1986.

[3] S. A. Cox, "Clock sensitivity reduction in echo cancellers," *Electron. Lett.*, vol. 21, no. 14, pp. 585-586, July 1985.

[4] S. Marcos, O. Macchi, and J. B. Pintaux, "Timing jitter effects in an echo canceller for full duplex data transmission," in *Proc. EUSIPCO '86*, The Hague, Sept. 1986, pp. 1145-1148.

[5] B. Widrow, J. M. McCool, M. G. Larimore, and C. R. Johnson, "Stationary and nonstationary learning characteristics of the LMS adaptive filter," *Proc. IEEE*, vol. 64, pp. 1151-1162, Aug. 1976.

[6] O. Macchi, "Optimization of adaptive identification for time-varying filters," *IEEE Trans. Automat. Contr.*, vol. AC-31, pp. 283–286, Mar. 1986.

[7] S. Marcos and O. Macchi, "Tracking capability of the least mean square algorithm: Application to an asynchronous echo canceller," *IEEE Trans. Acoust., Speech, Signal Processing*, vol. ASSP-35, pp. 1570–1578, Nov. 1987.

[8] L. E. Franks and J. P. Bubrouski, "Statistical properties of timing jitter in a PAM timing recovery scheme," *IEEE Trans. Commun.*, vol. COM-22, pp. 913–920, July 1974.

On the Symbol Error Probability of Maximum-Selection Diversity Reception Schemes Over a Rayleigh Fading Channel

GWO-TSUEY CHYI, JOHN G. PROAKIS, AND CATHERINE M. KELLER

Abstract—**This correspondence discusses the symbol error probability of two selection schemes, namely, maximum signal-to-noise ratio ($M\gamma$) selection and maximum output (MO) selection, for M-ary multidiversity reception over a Rayleigh fading channel. The symbol error probability of the MO scheme is lower than that of the $M\gamma$ scheme. The more diversity receptions used, the larger the difference. A simple expression of crossover average signal-to-noise ratio (per bit) is presented as a guideline for increasing the number of diversity receptions.**

I. INTRODUCTION

Multidiversity or multichannel reception is a classical and effective technique for combatting deep signal fades usually encountered in a single-diversity Rayleigh-fading channel. One acquires multiple replicas of a transmitted signal by using spaced receiving antennas and receivers by sending and receiving the same signal on several different carrier frequencies, or by transmitting the same signal several times over appropriately spaced time slots. The number of diversity receptions used is constrained by the limitations in space, frequency bandwidth, or throughput.

Multiple copies of the transmitted signal can also be introduced naturally at the receiver by the communication media and/or environment. For example, in ionospheric communication [1], land mobile communication [2], and indoor wireless communication [3], a large number of diversity receptions will hopefully be available for use.

There are several methods for doing multidiversity reception. Among all of them, selecting the best diversity reception is one of the simplest concepts [4, Sect. 10-4]. Most of the research on selection schemes was conducted in the fifties. For example, Bond and Meyer [5] considered the satisfactorily operating percentage of time for the cases where Rayleigh fading could appear either in signal or noise or both. They considered both the cases of selecting the maximum signal-to-noise ratio (SNR) and selecting the strongest signal-plus-noise diversity reception. In digital data transmission, Montgomery [6] studied three selection schemes with limiter-discriminator detection and one dual-filter signal-plus-noise selection scheme for binary frequency-shift keying with Rayleigh distributed carrier amplitude. Pierce [7] states that selecting the largest instantaneous signal is a nonoptimum combining scheme for noncoherent multidiversity reception over a slowly fading Rayleigh channel. He gives an expression for the bit error probability in the binary case. Leung [8] also shows the error rate expression in the binary case and gives an approximation of the optimum number of diversity receptions for a given SNR per bit. Recently, Kavehrad and Ramamurthi [3] studied the selection diversity operation in an indoor wireless communication environment.

In this correspondence, we study the M-ary symbol error probability for two maximum selection schemes, namely, maximum SNR ($M\gamma$) selection and maximum output (MO) selection. In Section II, we describe the system model. The error performance of the two schemes is studied in Section III. Furthermore, we define the crossover SNR, a parameter which can help determine the number of diversity receptions (diversity level) to use. We find a simple expression for the crossover SNR of the $M\gamma$ scheme in Section IV. Section V gives conclusions.

II. SYSTEM MODEL

Consider M-ary orthogonal signaling over an independently slowly fading Rayleigh, L diversity communication channel. Each signaling waveform in the symbol interval $[0, T)$ is equiprobable and contains the same energy $\mathcal{E}$. The received signal is contaminated by additive white Gaussian noise with two-sided power spectral density of height $N_0/2$. The noise on each diversity reception is assumed to be independent and identically distributed (iid). An optimum receiver for each diversity reception is a matched-filter followed by a square-law envelope detector [9, Sect. 7.6].

Let X_{km}, $m = 1, 2, \cdots, M$, be the output of the square-law detector for the mth symbol on the kth diversity channel. Suppose the first element in the symbol alphabet is sent. Then, X_{km} can be expressed as [10, Sect. 7.7]

$$X_{k1} = |2\mathcal{E}\alpha_k \exp(j\phi_k) + N_{k1}|^2 \quad (1)$$

$$X_{km} = |N_{km}|^2, \quad m = 2, 3, \cdots, M \quad (2)$$

where N_{km} is a zero-mean complex Gaussian random variable

Paper approved by the Editor for Fading, Dispersive, and Multipath Channels of the IEEE Communications Society. Manuscript received December 17, 1987; revised April 22, 1988.

The authors are with the Department of Electrical and Computer Engineering, Northeastern University, Boston, MA 02115.

IEEE Log Number 8824908.